TWO-DIMENSIONAL NUMERICAL SIMULATION OF THE EFFECT OF POROSITY ON THE COMPRESSIVE STRENGTH OF CONCRETE

Thanh Hai Nguyen*, Van Huong Nguyen

The University of Danang - University of Science and Technology, Vietnam

*Corresponding author: nthai@dut.udn.vn

(Received: April 27, 2025; Revised: June 10, 2025; Accepted: June 19, 2025)

DOI: 10.31130/ud-jst.2025.23(10C).676E

Abstract - Concrete is widely used in construction due to its versatility, durability, and low cost. Porosity, defined as the ratio of voids, significantly affects compressive strength. This study uses 2D numerical simulations with the discrete element method (DEM) and Voronoi tessellation to model internal voids, examining porosity from 1% to 15%. Results show that porosity strongly influences both compressive strength and strain in concrete. When porosity increases from 3% to 5%, the compressive strength decreases by 13–33%. Notably, at 15% porosity, the compressive strength is reduced by up to 80% compared to the 1% porosity case. Interestingly, both maximum compressive strength and strain show an exponential dependence on porosity. These findings highlight that, in addition to other material properties, porosity is a key factor in determining the compressive strength of concrete. This study aims to enhance understanding of concrete behavior, contributing to improved performance and sustainability in construction.

Key words - Compressive strength; concrete; porosity; discrete element method; Voronoi tessellation

1. Introduction

Concrete is one of the most popular materials in construction, used in buildings, dam hydraulics, infrastructure, due to its versatility, durability and low cost. Concrete is composed of coarse aggregates, cement mortar, interfacial transition zones (ITZ), and pores, that it can be considered a sustainable material. A comprehensive understanding of its mechanical behavior particularly compressive strength is critical for ensuring structural longevity. Compressive strength is influenced by numerous factors, including mix proportions, water-cement ratio, aggregate quality, compaction, curing conditions, and porosity. The influence of fine and coarse aggregate quantities on the properties of concrete was discussed in Maguesvari's work. In this experimental study, the fine aggregate increase from 20% to 40%, the compressive strength increases significant from 12 – 24 N/mm^2 [1], [2]. Similarly, Fan Yu et al. highlighted the influence of aggregate size and pore structure on compressive strength: while larger aggregates improve compressive strength, but compressive strength is sensitive to the irregularity of the pore structure [3]. Porosity, one of the critical factors affecting the mechanical properties of concrete, arises from air entrapment during mixing, inadequate compaction, or water evaporation [4], [5], [6], [7], [8]. Porosity significantly reduces the mechanical strength of concrete, as porosity increases, the volume of voids within the concrete matrix also increases, leading to a reduction in both compressive and tensile strength [9], [10]. Sohi et al. quantified this relationship, showing that voids degrade strength by up to 30% due to stress concentration and reduced load-bearing capacity [5], higher porosity leads to greater permeability but simultaneously reduces compressive strength [7], Li et al. further confirmed that porosity in both the ITZ and mortar matrix inversely correlates with compressive strength, emphasizing its role as a key performance determinant [8]. While experimental methods provide valuable insights, they are often time-consuming and costly for systematic porosity analysis. Numerical simulation is a better method and can be improved by changing parameters during the work, particularly the Discrete Element Method (DEM), offer a robust alternative by modeling concrete as discrete rigid particles (disks in 2D or spheres in 3D) bonded by cohesive forces [11] - [14]. For instance, Pieralisi et al. used DEM to model concrete under uniaxial compression and bending [15], while Wang et al. evaluated the role of aggregates in concrete strength [16]. However, existing DEM models often oversimplify pore structure by assuming spherical voids or predefined geometries, limiting their ability to mimic real-world porosity distributions.

To address this gap, an attractive approach in DEM modeling of concrete is the application of Voronoi tessellation technique. This technique partitions a plane into regions that are closest to each of a given set of objects. In the context of concrete modeling, Voronoi tessellation facilitates the straightforward generation of voids within the numerical sample [17]-[19]. Zhou et al. proposed an enhanced model based on this method, capable of representing porous structures with adjustable porosity levels [20]. While numerous studies have explored DEM simulation of concrete and the effect of porosity on compressive strength, systematic research on the influence of randomly removing Voronoi elements to create varying porosity on the compressive strength of concrete remains limited. Most existing models focus on simulating different components of concrete (such as aggregates, mortar, and ITZ) [15], [16] but few have specifically investigated the effect of randomly distributed pores in the range of 1–15% on the compressive strength of concrete.

In this paper, the discrete element method (DEM) is used to investigate the effects of the porosity on the compressive strength of concrete. These voids in all numerical models are generated using Voronoi tessellation by removing Voronoi elements.

2. Numerical approach and model setting

The discrete element method (DEM), in this paper, is used to investigate the effects of the porosity on the compressive strength of concrete. This method can be used to simulate the behavior of systems of particles such as granular materials, rock mechanics, and other discontinuous materials [21], [22], [23]. The interaction between the particles is characterized by the friction coefficient between them, as well as the coefficients of normal and tangential restitution. These particles are modeled as a rigid body and interact with each other under the contact force law. Notably, there is no overlap between particles during interaction. In order to investigate the effects of the porosity, the Voronoi tessellation is applied in this model to divide the particles into the rectangular box [24]. On the other hand, cohesion attraction between the particles is used to prevent their dispersion while allowing contact. Under the influence of external force, to make the compressive strength of concrete, the choice of contact interaction law between the particles is necessary. Here, we consider that the Signorini's conditions and the Coulomb's friction law are applied to illustrate the interaction. When two particles are in contact, a constant cohesion force f_c attracts them. The normal force is positive or negative when the distance between the particles or these particle velocities is zero as Figure 1a. Furthermore, Coulomb's friction law gives a relationship between the tangential force f_t and the sliding velocity v_t when a pair of particles is in contact, as illustrated in Figure 1b. Meanwhile, the tangential force f_t can vary within the range $[-\mu(f_n + f_c); \mu(f_n + f_c)]$ when v_t is zero. If v_t is nonzero, f_t is given by the friction coefficient μ times the normal force f_n.

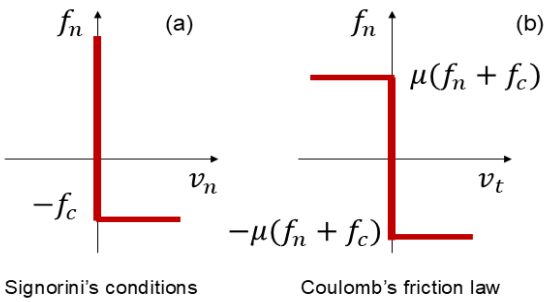

Figure 1. *Graph illustrating the contact law between the particles. (a) the Signorini's conditions in velocity, (b) the Coulomb's friction law*

To investigate the effects of the porosity on the compressive strength of the concrete, a sample composed of an assembly of rigid polygonal particles is created with dimensions of 150mm x 150mm according to the Vietnam National Standard TCVN 3118:2022. Extensive two-dimensional numerical simulations are performed on systems containing up to 5.000 polygonal particles. After randomly removing particles using Voronoi tessellation technique, the model with different porosities is created. The porosity n is defined by $\phi = 1 - \frac{V_i}{V_0}$, where V_i is the volume of the sample used in the model, V_0 = 150 x 150 (mm^2) is the initial volume. In this study, the porosity is set to ϕ (%) = 1, 3, 5, 7, 10, 12, and 15%. Figure 2 shows the uniaxial compression test of the concrete. The top wall descends at a steady rate of 90 N/s, while the bottom wall remains stationary.

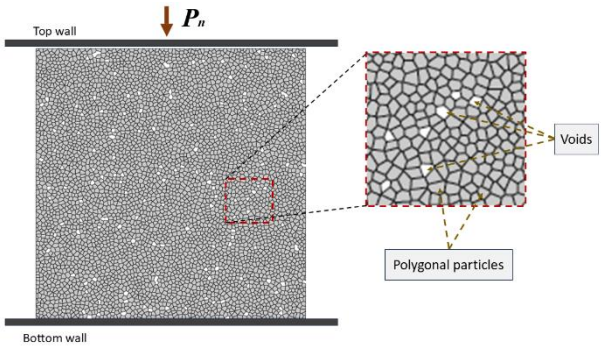

Figure 2. *Snapshot of the uniaxial compression of a concrete composed of the rigid polygonal particles and the voids*

The cohesion force f_c in all the numerical simulations is set to 0.55 (N), meanwhile this value is a maximum tensile force a pair of contacting particles. In this current work, the choice of this value f_c is critical since the deformation of the particle assembly is affected by the external force or the compressive load P_n during testing. If the cohesion force is too small, the particle assembly cannot achieve the desired compressive strength. All other parameters for this work are detailed in Table 1.

Table 1. *Principal parameters for the simulations*

Parameter	Symbol	Value	Unit
Number of rigid polygonal particles	N_p	4200 - 4950	-
Compression force	P_n	90	N/s
Maximum tensile force at contact	f_c	0.55	N
The porosity	ϕ	1, 3, 5, 7, 10, 12, 15	%
Density	ρ	2400	kg/m^3
Coefficient of friction	μ	0.5	
Time step	dt	1e-4	s

3. Results

According to the Vietnam National Standard TCVN 3118:2022 for hardened concrete – Test method for compressive strength, the size of the concrete sample in this work is set to 150mm x 150mm and the compressive load P_n increases at a constant rate of 90 N/s until the sample is destroyed.

Figure 3 illustrates the linear relationship between the compressive load and time for all the simulations of different porosities. The load continuously increases until the sample is destroyed, following the progression of the time. The results show that the effects of the porosity are significant. The maximum load is around 3 (kN) for the 1% case after 33 seconds. However, as the porosity n increases, the other samples fail with smaller load values at corresponding times (see Figure 3). This influence may be explained by the increase in voids, which leads to a decrease in the sample's compactness and a reduction in its

compressive strength. On the other hand, in addition to the compactness of sample, the cohesion force between the particles plays an important role in helping the sample maintain until it is destroyed.

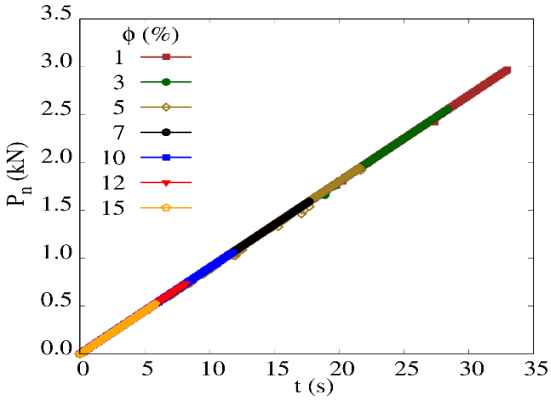

Figure 3. *Compressive load as a function of the time*

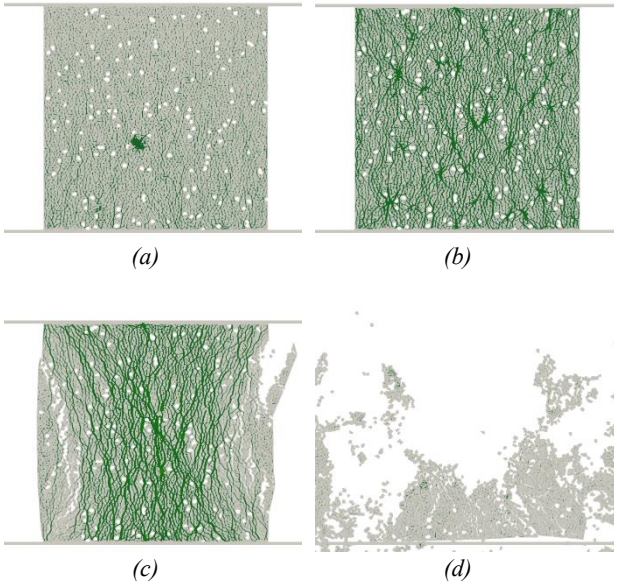

Figure 4. *Snapshots of the numerical simulation for a porosity 3%. (a) the initial stage, (b) strain at ε_{yy} = 0.01 %, (c) at ε_{yy}= 0.07 %, (d) concrete damage. The gray color represents particles, and the green lines indicate the normal force*

Under the continuously increasing load, the sample deforms over time. Figure 4 shows the process of uniaxial compression of the concrete with a porosity of 3%, in which, (a) shows the first-time step, where the normal force is distributed onto the sample with green lines. As the load increases, the concrete sample, composed of polygonal particles will begin to deform until it is damaged, as shown in (b), (c), and (d). Specifically, the normal force is distributed in the vertical direction of the impacted load, and the thickness of the lines is proportional to the magnitude of the force. The strain ε_{yy} is defined by:

$$\varepsilon_{yy} = \frac{\Delta h_i}{h_0} = \frac{h_0 - h_i}{h_0} \left(\frac{mm}{mm}\right) \quad (1)$$

where h_0 is the initial height and is equal to 150mm, h_i suggests the height instant during the simulation.

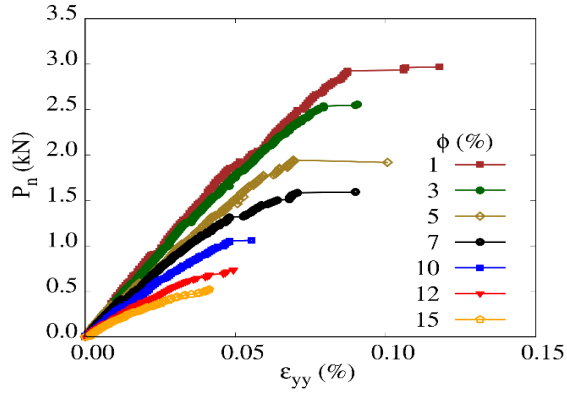

Figure **5** shows the compressive load as a function of the strain for all sample tests. The results show the sample with a larger void is destroyed earlier, within the range of 0.0004 to 0.0005 of strain. Conversely, the strain value is higher for the cases with a smaller porosity. This difference may originate from the compactness of the assembly of polygonal particles.

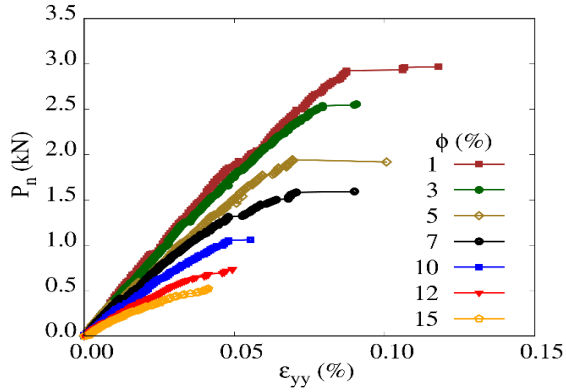

Figure 5. *Compressive load as a function of the vertical deformation*

Furthermore, although the load value continues to increase due to the numerical model not stopping, the compressive strength is determined when the sample has been damaged. The compressive strength can be defined as:

$$R = \alpha \times \frac{P_n}{A} \left(\frac{kN}{mm^2}\right) \quad (2)$$

$$q = \alpha \times \frac{P_n}{a} \left(\frac{kN}{mm}\right) \quad (3)$$

In equations 2 and 3, R and A represent the compressive strength and the area of sample subjected to the load (mm^2) in the 3D sample, respectively, while q and a denote the compressive strength and the length of sample subjected to the load (mm) in the current work. α is the change coefficient, set to 1.0 for a sample size of 150mm x 150mm.

Figure 6 displays the compressive strength of concrete q as a function of strain ε_{yy}. In fact, the observed results indicate that the effects of the porosity on the compressive strength of the concrete composed of an assembly of polygonal particles are significant. The compressive strength decreases as the porosity increases. As explained above, when the load continues to increase, the sample

with a higher porosity tends to fail earlier than the one with a lower porosity. Therefore, the maximum compressive strength obtained also depends on the sample's porosity.

In this current work, a concrete model composed of an assembly of polygonal particles with porosities ranging from 1% to 15% were investigated. When the porosity varies from 3% to 5%, the compressive strength is reduced by 13% to 33% compared to the 1% case. When the porosity varies from 12% to 15%, the uniaxial compressive strength is reduced by 70% to 80% compared to the case of 1%. Particularly, while the porosity increases from 1% to 5%, the compressive strength is reduced by 33%, with higher of the porosities, the compressive strength continues to decrease.

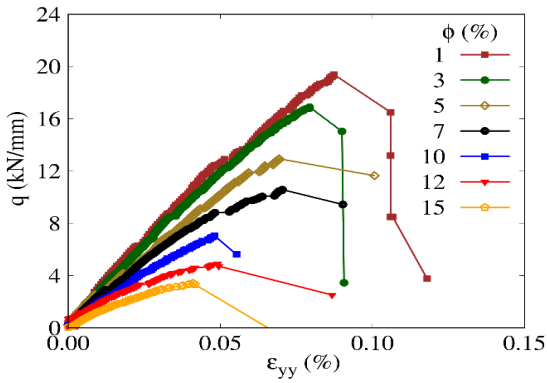

Figure 6. *The effect of the porosity on the compressive strength of concrete composed of an assembly of polygonal particles*

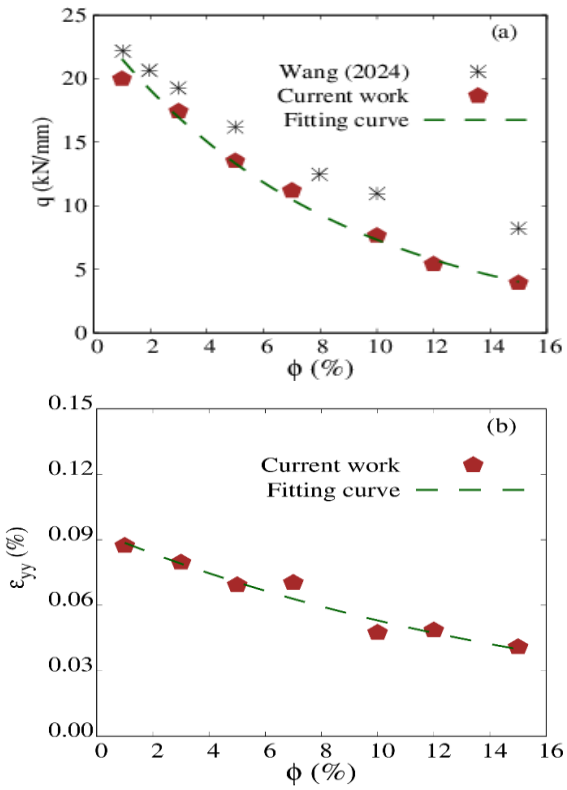

Figure 7. *Maximum values of vertical compressive strength and vertical deformation as a function of the porosity*

To highlight the effect of the porosity on the compressive strength, the maximum value of vertical compressive strength q and vertical deformation ε_{yy} are measured. Figure 7 shows the compressive strength of concrete and strain as a function of the porosity. Figure 7(a) and (b) present the relationship between q vs. ϕ and ε_{yy} vs. ϕ, obtained from all simulations. A comparison is made with the results of Wang et al., as shown in Figure 7(a). Notably, Wang's model investigated the influence of porosity using the finite element method. The difference between the two results may arise from the fact that this work employs a fixed cohesion value of f_c = 0.55 N. Furthermore, an increase in porosity leads to a reduction in the number of elements, which consequently results in a greater decrease in strength.

The results indicate in this study that when porosity increases, the relationship between porosity and the compressive strength, as well as the strain, follows an exponential relationship, as shown in equations 4 and 5. These exponential functions fit well, with R^2 = 98% for the compressive strength and R^2 = 95% for the strain.

$$q = 24.3e^{-0.12\phi} \quad (4)$$

$$\varepsilon_{yy} = 0.094e^{-0.057\phi} \quad (5)$$

According to the above results, the porosity of 1% corresponds to the uniaxial compressive strength of the concrete B15 at 19.8 (kN/mm) corresponding to TCVN. Finding this relationship is very helpful for predicting the compressive strength of concrete corresponding to the different porosity, as well as the level of uniaxial deformation.

4. Conclusion

In this work, the influences of the porosity on the compressive strength of the concrete are investigated using discrete element method technique. The Voronoi tessellation is applied to create the voids in the concrete sample. The concrete sample, composed of an assembly of rigid polygonal particles, has dimensions of 150mm x 150mm, according to Vietnam National Standard. Under a continuously increasing load to 90 N/s, the concrete sample with different porosities ranging from 1% to 15% is deformed until the sample is damaged.

The numerical results show that the mechanical behavior of concrete is highly dependent on the porosity. Concrete samples with a higher porosity are destroyed more quickly than those with a lower porosity, leading to a smaller level of deformation. Specifically, a sample with a 15% porosity is destroyed in just 5 seconds, while it takes more than 33 seconds for a sample with a 1% porosity to fail. Furthermore, the compressive strength of concrete is influenced by the porosity, while the porosity increases from 3% to 5%, the compressive strength decreases by 13 - 33% compared to the sample with a 1% porosity. Notably, when the porosity reaches 15%, the compressive strength drops by up to 80% compared to the initial 1% value. The results obtained indicate that as the porosity increases from 1% to 5%, the compressive strength is reduced by 33%, and the compressive strength continues to decrease with a higher porosity. This difference may be deeply explained by a microscopic level, characterized by the distribution of

the normal force between the polygonal particles and the compaction of systems play key roles. The numerical findings also reveal that both the maximum vertical compressive strength and maximum strain follow an exponential relationship with the porosity, as shown in equations 4 and 5, respectively. The results presented in this current work significantly complement a better understanding of the effects of porosity on the compressive strength of concrete. This study examines the effects of porosity on the compressive strength of concrete. Further work should explore the effects of mix proportions, aggregate quality, and friction between wall and sample during compression. A similar investigation could also be extended to 3D sample test, enabling a more comprehensive understanding of the practical applications.

REFERENCES

[1] M. U. Maguesvari and V. L. Narasimha, "Studies on Characterization of Pervious Concrete for Pavement Applications," *Procedia Soc Behav Sci*, vol. 104, pp. 198–207, Dec. 2013, doi: 10.1016/j.sbspro.2013.11.112.

[2] O. Babatola and C. Arum, "Determination of the Compressive Strength of Concrete from Binary Cement and Ternary Aggregates," *Open Journal of Civil Engineering*, vol. 10, no. 04, pp. 385–402, 2020, doi: 10.4236/ojce.2020.104029.

[3] F. Yu, D. Sun, J. Wang, and M. Hu, "Influence of aggregate size on compressive strength of pervious concrete," *Constr Build Mater*, vol. 209, pp. 463–475, Jun. 2019, doi: 10.1016/j.conbuildmat.2019.03.140.

[4] Z. Xu, N. Xu, and H. Wang, "Effects of Particle Shapes and Sizes on the Minimum Void Ratios of Sand," *Advances in Civil Engineering*, vol. 2019, 2019, doi: 10.1155/2019/5732656.

[5] A. Sohi, S. S. Roudari, S. Hamoush, M. C. Ahmed, T. M. Abu-Lebdeh, and T. M. Abu-Lebdeh INFLU-, "Influence of void's sizes and locations on the concrete compressive strength," *3rd European and Mediterranean Structural Engineering and Construction Conference*, pp. 1–11, 2021, [Online]. Available: https://hal.science/hal-03092350v1.

[6] Y. Wang, T. Liang, and F. Jin, "Void effect study on the compressive behavior of RFC based on the 3D four-phase mesoscopic finite element model," *Constr Build Mater*, vol. 417, Feb. 2024, doi: 10.1016/j.conbuildmat.2024.135145.

[7] C. Sánchez-Mendieta, J. J. Galán-Díaz, and I. Martinez-Lage, "Relationships between density, porosity, compressive strength and permeability in porous concretes: Optimization of properties through control of the water-cement ratio and aggregate type," *Journal of Building Engineering*, vol. 97, Nov. 2024, doi: 10.1016/j.jobe.2024.110858.

[8] Y. Peng, L. Su, Y. Wang, and L. Zhang, "Analysis of the Effect of Porosity in Concrete under Compression Based on DIP Technology," *Journal of Materials in Civil Engineering*, vol. 34, no. 1, Jan. 2022, doi: 10.1061/(ASCE)MT.1943-5533.0004011.

[9] Z. Zhang and H. Wang, "The pore characteristics of geopolymer foam concrete and their impact on the compressive strength and modulus," *Front Mater*, vol. 3, Aug. 2016, doi: 10.3389/fmats.2016.00038.

[10] J. Shan, J. He, and F. Li, "Numerical Simulation of Pervious Concrete Based on Random Pore Model," *Advances in Civil Engineering*, vol. 2020, 2020, doi: 10.1155/2020/8831506.

[11] Y. Yu, Y. Zheng, and X. Y. Zhao, "Mesoscale modeling of recycled aggregate concrete under uniaxial compression and tension using discrete element method," *Constr Build Mater*, vol. 268, Jan. 2021, doi: 10.1016/j.conbuildmat.2020.121116.

[12] J. Zhou, M. Zheng, Q. Zhan, R. Zhou, Y. Zhang, and Y. Wang, "Discrete element modelling of the uniaxial compression behavior of pervious concrete," *Case Studies in Construction Materials*, vol. 18, Jul. 2023, doi: 10.1016/j.cscm.2023.e01937.

[13] M. T. Tien, N. Do Tu, X. V. Hong, and Emmanuel Ferrier, "A 2-D numerical model of the mechanical behavior of the textile-reinforced concrete composite material: effect of textile reinforcement ratio," *Journal of Mining and Earth Sciences*, vol. 61, no. 3, pp. 28–37, Jun. 2020, doi: 10.46326/JMES.2020.61(3).04.

[14] J. Raisianzadeh, A. A. Mirghasemi, and S. Mohammadi, "2D simulation of breakage of angular particles using combined DEM and XFEM," *Powder Technol*, vol. 336, pp. 282–297, Aug. 2018, doi: 10.1016/j.powtec.2018.06.006.

[15] R. Pieralisi, S. H. P. Cavalaro, and A. Aguado, "Discrete element modelling of mechanical behaviour of pervious concrete," *Cem Concr Compos*, vol. 119, May 2021, doi: 10.1016/j.cemconcomp.2021.104005.

[16] P. Wang, N. Gao, K. Ji, L. Stewart, and C. Arson, "DEM analysis on the role of aggregates on concrete strength," *Comput Geotech*, vol. 119, Mar. 2020, doi: 10.1016/j.compgeo.2019.103290.

[17] G. Frenning, "Efficient Voronoi volume estimation for DEM simulations of granular materials under confined conditions," *MethodsX*, vol. 2, pp. e79–e90, 2015, doi: 10.1016/j.mex.2015.02.004.

[18] E. A. Lazar, J. Lu, C. H. Rycroft, and D. Schwarcz, "Characterizing structural features of two-dimensional particle systems through Voronoi topology," *Model Simul Mat Sci Eng*, vol. 32, pp. 1–20, Jun. 2024, doi: 10.1088/1361-651X/ad8ad9.

[19] C. Flack and D. Dinkler, "A multifield discrete element model for concrete," *Comput Part Mech*, 2024, doi: 10.1007/s40571-024-00883-z.

[20] Y. Zhou, P. Isaksson, and C. Persson, "An improved trabecular bone model based on Voronoi tessellation," *J Mech Behav Biomed Mater*, vol. 148, Dec. 2023, doi: 10.1016/j.jmbbm.2023.106172.

[21] S. Nezamabadi, T. H. Nguyen, J. Y. Delenne, and F. Radjai, "Modeling soft granular materials," *Granul Matter*, vol. 19, no. 1, pp. 1–12, 2017, doi: 10.1007/s10035-016-0689-y.

[22] T. H. Nguyen, "Uniaxial compression a soft grain composed of aggregate primary particles," *The University of Danang - Journal of Science and Technology*, pp. 48–52, Jan. 2025, doi: 10.31130/ud-jst.2025.495E.

[23] T.-H. Nguyen, T.-V. Ngo, and T.-T. Vo, "Combined Inter-Particle and Wall-Particle Friction Coefficient Effects on Collapse Mobility and Deposition Morphology of a Granular Column Composed of Pentagonal Grains," *Mechanics of Solids*, 2025, doi: 10.1134/S0025654425600618.

[24] X. Tan, M. Zhao, Z. Zhu, and Y. Jin, "Elastic Properties Calibration Approach for Discrete Element Method Model Based on Voronoi Tessellation Method," *Geotechnical and Geological Engineering*, vol. 37, no. 3, pp. 2227–2236, Jun. 2019, doi: 10.1007/s10706-018-0682-9.